Send Orders for Reprints to reprints@benthamscience.net

*Current Pharmaceutical Design*, 2024, *30*, 1610-1623

RESEARCH ARTICLE

# Green Synthesis of Silver Nanoparticles using *Cirsium congestum* Extract Modified by Chitosan/Alginate: Bactericidal Activity against Pathogenic Bacteria and Cytotoxicity Analysis in Normal Cell Line

Mahnaz Mohtashami[1], Alieh Rezagholizade-Shirvan[2], Zahra Hojati Bonab[3], Mohammad Reza Amiryousefi[2,*], Majid Darroudi[4], Mobina Sadat Ahmadi Solimani[1], Sajad Yaghoobi[5], Samaneh Dolatabadi[1], Ahmad Ghasemi[6,*] and Amir Abbas Momtazi-Borojeni[7,8,*]

[1]*Department of Microbiology, School of Basic Science, Islamic Azad University, Neyshabur Branch, Neyshabur, Iran;* [2]*Department of Food Science and Technology, Neyshabur University of Medical Sciences, Neyshabur, Iran;* [3]*Department of Microbiology, School of Basic Science, Islamic Azad University, Bonab Branch, Bonab, Iran;* [4]*Nuclear Medicine Research Center, Mashhad University of Medical Sciences, Mashhad, Iran;* [5]*Department of Basic Medical Sciences, Neyshabur University of Medical Sciences, Neyshabur, Iran;* [6]*Department of Biochemistry, Nutrition and Food Sciences, School of Medicine, Gonabad University of Medical Sciences, Gonabad, Iran;* [7]*Healthy Ageing Research Centre, Neyshabur University of Medical Sciences, Neyshabur, Iran;* [8]*Department of Medical Biotechnology, School of Medicine, Neyshabur University of Medical Sciences, Neyshabur, Iran*

ARTICLE HISTORY

Received: January 17, 2024
Accepted: March 09, 2024

*DOI:*
*10.2174/0113816128304460240408085736*

**Abstract:** ***Aim*:** The study aimed to determine *in vitro* pharmacological effects of modified Ag nanoparticles (AgNPs).

***Background*:** AgNPs are considered antimicrobial agents. However, the cytotoxicity of chemically synthesized AgNPs (cAgNPs) has raised challenges that limit their use.

***Objective*:** The purpose of the study was to examine the antimicrobial and cytotoxicity effects of AgNPs synthesized using *Cirsium congestum* extract modified by chitosan/alginate AgNPS (Ch/ALG-gAgNPs).

***Methods*:** Nanoparticles were characterized using TEM, DLS, XRD, and FTIR. Resistant strains of *Escherichia coli* (*E. coli*) and *Staphylococcus aureus* (*S. aureus*) were used for the antimicrobial analysis of Ch/ALG-gAgNPs using disc diffusion and microdilution methods. The effects of NPs on cell viability and apoptosis in L929 normal cells were determined using MTT assay and annexin/PI staining, respectively.

***Results*:** Physicochemical characterizations confirmed Ch/ALG-gAgNPs to be spherical and uniformly dispersed, and their size ranged from 50 to 500 nm. Ch/ALG-gAgNPs inhibited the growth of microbial strains in a dose-dependent manner. The antibacterial effect of Ch/ALG-gAgNPs was significantly higher than cAgNPs. The Ch/ALG-gAgNPs showed little cytotoxicity against normal cells at concentrations less than 50 µg/ml. Cytotoxicity effects of Ch/ALG-gAgNP were less than cAgNPs. Flow cytometry and real-time PCR results showed a decrease in apoptosis percentage and BAX marker in the presence of Ch/ALG-gAgNPs relative to when the cell was treated with cAgNPs.

***Conclusion*:** Current findings introduce novel gAgNPs modified with chitosan/alginate for use in medicine.

**Keywords:** Green synthesis, chitosan, alginate, antibacterial activity, cytotoxicity, cell apoptosis.

## 1. INTRODUCTION

Metal-based nanoparticles have gained tremendous interest in biomedical and industrial fields [1-5]. In this regard, Silver Nanoparticles (AgNPs) have been demonstrated to show good stability, conductivity, and provide anti-bacterial, anti-fungal, anti-cancer, wound healing, and anti-inflammatory activities [6]. In biomedical applications, AgNPs are used in antiseptic, therapeutic, and diagnostic approaches [6, 7]. Cytotoxic effects of metal-based nanoparticles on human normal cells is a critical challenge for their use in biomedicine [8]. In this respect, numerous toxicological analyses on animal models have reported the adverse effects of AgNPs on the skin, lungs, blood cells, brain, liver, ovaries, and gonads by inducing cell apoptosis, necrosis, and genetic mutations [7]. Therefore, the development of cost-effective, biocompatible, and safe approaches to synthesizing non-toxic AgNPs is required. Cytotoxicity of AgNPs may be attributed to the high tendency of nanoparticles to aggregate and precipitate in aqueous environments [8]. In the presence of electrolytes, the aggregative stability of silver dispersions is markedly decreased, and thus, colloidal stability of AgNPs is reduced [9, 10]. In the biological media, electrostatic forces and steric hindrances between AgNPs are attenuated and nanoparticles

*Address correspondence to these authors at the Department of Food Science and Technology, Neyshabur University of Medical Sciences, Neyshabur, Iran;
E-mail: YousefiAA3@mums.ac.ir (M.R.A.); Department of Biochemistry, Nutrition and Food Sciences, School of Medicine, Gonabad University of Medical Sciences, Gonabad, Iran; Fax: 05142627524; E-mail: Ghasemia2@nums.ac.ir (A.G.); Healthy Ageing Research Centre, Neyshabur University of Medical Sciences, Neyshabur, Iran; Department of Medical Biotechnology, School of Medicine, Neyshabur University of Medical Sciences, Neyshabur, Iran; Fax: 05142627524;
E-mail: abbasmomtazi@yahoo.com (A.M.-B.)

1873-4286/24 $65.00+.00 

are able to agglomerate more readily [6]. The stability improvement of silver dispersions in the aqueous environments is required to prevent their aggregation and enhance their use in biomedicine. Surface modification (coating) with synthetic polymers is one of the most widely used approaches to promote the colloidal stability and safety of AgNPs [10-12]. The addition of synthetic polymers to AgNPs produces surface-charged nanoparticles, stabilizes silver dispersions, and increases their ability to enter and accumulate into cells by interaction with biomolecules [6, 13]. Nanoparticle coating inhibits the release of toxic ions from nanoparticles into biological media and protects them against oxidization [14]. Therefore, surface modification of nanoparticles minimizes their cytotoxicity and improves their efficacy for use in biomedicine [14]. In addition, the coating of AgNPs with non-cytotoxic polymers has been found to enhance the antimicrobial effects and reduce cytotoxicity in normal cells [15, 16].

Chitosan and alginate are natural polymers that have been widely used in surface modification of NPs [17]. Chitosan is biocompatible and inserts a polymer of great promise for surface modification of AgNPs [18, 19]. In the last two decades, this natural polymer has attracted the attention of researchers for its application in biomedicine due to its antimicrobial, anticancer, antioxidant, immunoenhancing, and antioxidant properties [19, 20]. Coating of the nanoparticles with chitosan can improve the physicochemical and biological properties of synthesized NPs and make them suitable for biological applications [21]. In this regard, several studies have reported successful coating of metal NPs using chitosan [22-28]. Moreover, alginate is a carbohydrate polymer composed of α-D-mannuronic acid and β-L-guluronic acid residues [29]. Likewise, chitosan and alginate have important biological properties, such as mucoadhesiveness, biodegradability, and biocompatibility, which enable them to serve as promising agents for use in medicine [17, 30-32]. In several studies, chitosan-alginate hydrogels have been synthesized to be used in biomedical applications [26, 27]. The electrostatic interactions between cationic groups of chitosan and the anionic groups of alginate provide a safe, degradable, and cost-effective polyelectrolyte complex [27]. In addition, composites formed from chitosan-alginate complex and AgNPs have shown strong bactericidal and anticancer effects [27, 28]. Of note, the green synthesis of AgNPs has gained significant attraction in recent years because of the requirement for environmentally friendly and cost-effective synthesis procedures [33-35]. Using the green routes, AgNPs are produced by using extracts of bacteria, fungi, alga, and plants instead of chemical-reducing agents [35]. Extracts of microorganisms and plants contain some bioactive compounds that can convert $Ag^+$ into AgNPs [36]. The use of plant extracts as reducing agents leads to the formation of AgNPs with unique properties and potential biomedical applications [33, 34]. AgNPs synthesized using plant extracts show lower cytotoxicity against normal cells and more stability in biological media, and have higher uniformity in size relative to NPs synthesized by chemical methods [36, 37].

*Cirsium congestum* (*C. congestum*), a plant species belonging to the family Asteraceae, has been reported to have different biological substances, such as flavonoids, polyphenols, semialdehyde, sabinene, and myrcene, which possess strong reducing properties [38, 39]. The *C. congestum* essential oil and its extract have shown potent antibacterial effects [38] and antioxidant activity [39]. However, no reports on the green synthesis of AgNPs using the *C. congestum* extract are available. In the present study, we, for the first time, have synthesized green AgNPs (gAgNPs) using *C. congestum* extract. In addition, chitosan and alginate polymers have been used for coating gAgNPs and synthesizing chitosan/alginate-modified gAgNPs (CS/ALG-gAgNPs). Besides, the antimicrobial, cytotoxicity, and antiapoptotic effects of Ch/ALG-gAgNPs against normal human cells (L929) have been evaluated in combination with non-coated AgNPs.

## 2. MATERIALS AND METHODS

Chitosan (low molecular weight, DDA 80%), sodium Tripolyphosphate (TPP), medium viscosity sodium Alginate (ALG) (Mw of $8\times10^4$-$12\times10^4$ g/mol), silver nitrate ($AgNO_3$), glacial acetic acid, calcium chloride ($CaCl_2$), hydrochloric acid (HCl), and other chemicals and reagents were of analytical grade and purchased from Merck (Darmstadt, Germany). All cell culture media and MTT [3-(4,5-dimethyl thiazole-2-yl)-2,5-diphenyl tetrazolium] were purchased from Sigma-Aldrich (USA).

### 2.1. Preparation of *C. congestum* Extract

We obtained *C. congestum* plant from Neyshabur, Khorasan Razavi Province, Iran. To obtain an extract from *C. congestum*, two grams of plant bark were combined with 100 mL of distilled water. The mixture was then heated to 60°C and stirred for two hours. The resultant solution was filtered using Whatman No.1 filter paper (12.5 cm, UK). The filtered, clear solutions were kept at 4°C for use in green synthesis of AgNPs.

### 2.2. Green Synthesis of AgNPs using *C. congestum* Extract

Green synthesis of AgNPs using *C. congestum* was performed according to the following procedure: after extract preparation, 30 ml of *C. congestum* extract (20 mg/ml) was slowly mixed with approximately 100 ml of $AgNO_3$ (10 mM, Sigma-Aldrich, Germany) at 25°C with vigorous stirring at 1000 rpm for 48 hours. The color of the mixture changed from green to black or dark brown when *C. congestum* extract was mixed with $AgNO_3$ solution. This color change confirmed the reduction of $Ag^+$ ions by *C. congestum* extract to form stable gAgNPs in an aqueous medium. The gAgNPs solution was centrifuged at 15000 rpm for 5 minutes, was dried under vacuum, and was kept at 4°C until the next use.

### 2.3. Preparation of Chitosan/Alginate Mixture

The Chitosan/sodium Tripolyphosphate (Ch/TPP) solution was synthesized based on the ionic gelling method according to the protocol defined in the previous study [40]. Briefly, 0.5 g of chitosan powder was dissolved in 50 ml of acetic acid solution (%1) to obtain a chitosan solution (0.2% w/v) at room temperature using a continuous magnet stirrer. The obtained solution was filtered through a 0.22 μm size filter to remove any large and insoluble particles. Then, the TPP solution (1.0% w/v), as a crosslinker agent, was mixed with Ch solution under stirring at 350 rpm for 24 hours. Afterward, the sodium Alginate (ALG) solution (0.1% w/v) was added dropwise to the Ch solution to prepare the Chitosan/Alginate mixture (Ch/ALG) in a ratio of 2.0: 1.0 at room temperature under stirring at 350 rpm for 4 hours, followed by the addition of calcium chloride (10 mM) as a crosslinking agent to Ch/ALG mixture. Finally, the Ch/ALG mixture was washed 3 times with deionized water and stored at 4°C until needed [41].

### 2.4. Preparation of gAgNPs Modified by Ch/ALG

In this study, the freshly prepared AgNPs from *C. congestum* extract were further loaded onto the Ch/ALG particles. Briefly, the equivalent volume of gAgNPs (50 ml, 10 mM) was added to CS/ALG solution under stirring at 500 rpm for 6 hours. The mixture was then treated with ultrasound for 30 minutes to form a homogeneous solution. The homogeneous solution was centrifuged at

a speed of 10,000 r/min, and the sediment obtained was washed three times with deionized water and dried at 70°C.

### 2.5. Characterization of Ch/ALG- gAgNPs

According to previous studies, an absorption band in the region 400-450 nm demonstrated the formation of AgNPs [38]. In the present investigation, an Ultraviolet-visible (UV-Vis) spectrophotometer (CECIL brand, model CE9500) was used to scan the UV-Vis spectrum in the wavelength range of 200 to 800 nm with a resolution of 1 nm. FTIR (Thermo Nicolet, AVATAR370 FT-IR brand, USA) analysis was used to analyze the functional groups of plant extract, chitosan, alginate, gAgNPs, and Ch/ALG-gAgNPs in the range of 400-4000 $cm^{-1}$. The size and morphology of Ch/ALG-gAgNPs were determined using Transmission Electron Microscopy (TEM, Zeiss 100 kv, Model TEM Leo906) and Dynamic Light Scattering (DLS). X-ray Diffraction analysis (XRD, XPert Pro model, Netherlands) was used to assess the crystal structure and reflection level of Ch/ALG-gAgNPs.

### 2.6. Biological Experiments

#### *2.6.1. Antimicrobial Assay*

The disc diffusion experiment was used to examine the antibacterial effects of Ch/ALG mixture, cAgNPs [7], and Ch/ALG-gAgNP against antibiotic-resistant strains of *Escherichia coli* (ATCC 25,922) and *Staphylococcus aureus* (ATCC 25,923). Briefly, aliquots (100 µL) of overnight cultures of different bacterial strains were plated on Mueller-Hinton Agar (MHA). The agar plates were covered with sterilized filter paper discs, filled with various concentrations (0, 50, 100, 200 µg/ml) of cAgNPs or Ch/ALG-gAgNPs or Ch/ALG mixture (dissolved in water), and incubated at 37°C for 24 hours. Finally, the inhibition zone diameter (mm) around each test sample was measured and noted. The discs filled with standard antibiotics, such as gentamycin (10 mg/disc) and vancomycin (30 mg/disc), were also tested as the positive control. Water was used as a negative control. In the next experiment, 0.5 McFarland standard ($1\times10^8$ CFU/mL) of each tested strain was used to determine the Minimum Inhibitory Concentration (MIC) and Minimal Bacterial Concentration (MBC). For this, a 100 µL aliquot of each tested bacterial strain was mixed with an equal volume of treatments in a 96-well ELISA plate. After 24 hours of incubation at 37°C, MIC was determined by reading Optical Density (OD) at 600 nm. In addition, the MBC was determined by subculturing 100 µl of each well onto MH agar plates.

#### *2.6.2. Cell Culture*

The mouse fibroblast cell line (L929) was obtained from the National Cell Bank (NCBI, Pasteur Institute of Iran). The normal cells were grown in Dulbecco's Modified Eagle Medium (DMEM) supplemented with 10% Fetal Bovine Serum (FBS) as well as 100 U/mL penicillin and 100 g/mL streptomycin. The cells were incubated at 37°C in a humidified incubator with 95% humidity and 5% $CO_2$.

#### *2.6.3. Cytotoxicity Analysis of Ch/ALG-gAgNPs*

The 3-(4,5-dimethylthiazol-2-yl)-2,5-diphenyltetrazolium bromide (MTT) test was used to assess the effects of NPs on the viability of normal cells. L929 cells were seeded on a 96-well plate with complete media at a density of $5\times10^3$ cells/well and incubated at 37°C overnight. The cells were then treated with increasing concentrations (50-200 µg/mL) of cAgNPs or Ch/ALG-gAgNPs for 48 hours. Following 4 hours of incubation with MTT (2 µg/mL), MTT solutions were replaced with Dimethyl Sulfoxide (DMSO) to dissolve the formazan crystals. Finally, the absorbance of each test sample was measured at 570 nm, and cell viability was calculated by the following equation:

% cell viability = (absorbance of treated cells)/(absorbance of control cells) *100

#### *2.6.4. Flow Cytometry*

Quantification of early apoptosis, late apoptosis, and cell necrosis in cells ($1\times10^6$ cells per well) treated with 50 µg/mL of cAgNPs or Ch/ALG-gAgNPs (24 hours) was performed by flow cytometry. After incubation with the mentioned treatments, cells were harvested and stained using Annexin V-FITC/PI (Annexin-VFLUOS staining kit, Mannheim, Germany) for 15 min at room temperature. Forward scatter and side scatter of samples were measured after samples were run on FACS Calibur flow cytometer (Becton Dickinson, Mountain View, CA, USA), and analyzed using Cell Quest software (Becton Dickinson).

#### *2.6.5. Real-time PCR*

To confirm flow cytometry results, mRNA gene expression analysis of apoptosis markers (BAX and Bcl2) using Real-time PCR in the presence of 50 µg/ml of NPs was conducted. After total RNA extraction of L929 cells treated with cAgNPs or Ch/ALG-gAgNPs, the cDNA was synthesized using an Excel RT reverse transcriptase kit (RP1300, SMOBIO, Hsinchu City, Taiwan). The synthesized cDNA of all samples was used as the template for quantitative RT-PCR using the SYBR Green kit (Amplicon) on an ABI 7500 sequence detection system (Applied Biosystems). Reactions were performed using 96-well plates according to appropriate conditions by employing specific primers [42]. The gene expression analysis of target genes was quantified relative to GAPDH using $2^{-\Delta\Delta Ct}$ methods [43].

### 2.7. Statistical Analysis

The data are shown as the mean and SD of three separate trials. The differences between the groups were determined by one-way Analysis of Variance (ANOVA) coupled with the Tukey post-hoc test using the SPSS 22.0 program (IBM, USA). Statistical significance was defined as a *P*-value of 0.05.

## 3. RESULTS

### 3.1. Nanoparticle Synthesis and Characterization

In this study, *C. congestum* extract was used to synthesize gAgNPs, and then the Ch/ALG mixture was used for surface modification and to produce Ch/ALG-gAgNPs. The colorless silver nitrate solution incubated with *C. congestum* extract changed to brown due to nanoparticle formation (Fig. **1A**). UV-vis spectroscopy showed a broad peak between 400-450 nm by UV-vis spectrum, which confirmed gAgNPs formation (Fig. **1B**). The size and morphology of Ch/ALG-gAgNPs were evaluated using TEM and DLS. The TEM micrograph Ch/ALG-gAgNPs showed a spherical shape and loosely agglomerated NPs (Fig. **2A**). The DLS diagram revealed Ch/ALG-gAgNPs to have particle sizes measured in the range of 50 to 500 nm with an average size of 100 nm (Fig. **2B**). XRD pattern of the Ch/ALG-gAgNPs showed the 2θ angles of 38.2°, 46.57°, 64.5°, and 77.04° attributed to (111), (200), (220), and (311) crystal shapes of NPs involving a cubic structure. In addition, the diffraction peak at 2θ angle of 32.6 was attributed to the impurity of $Ag_2O$ in the nanoparticle sample (Fig. **2C**).

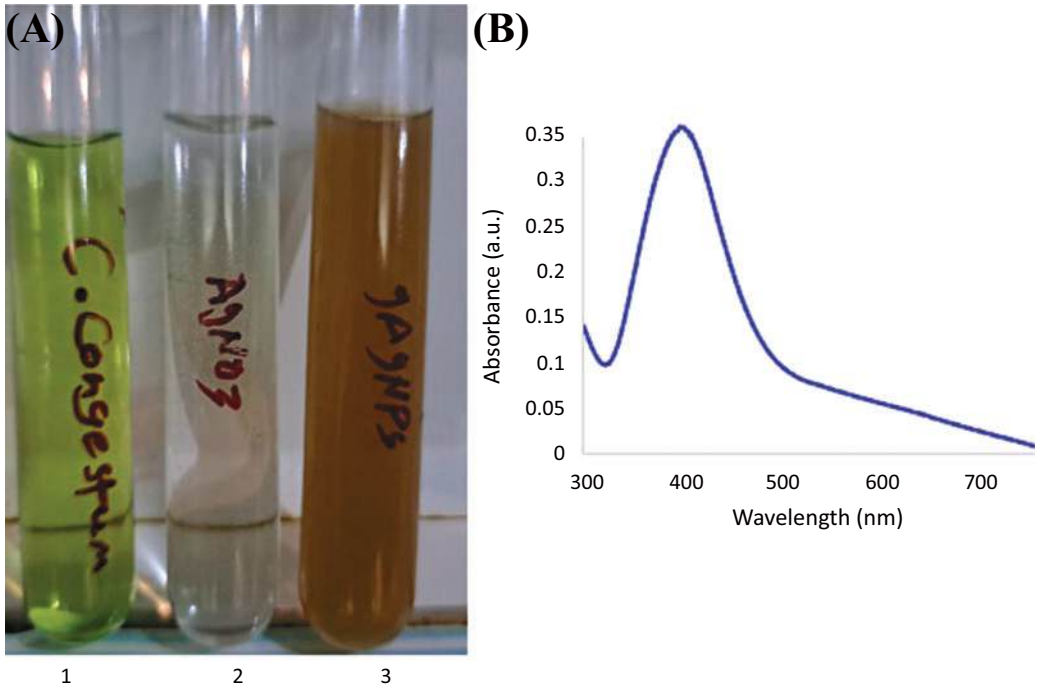


**Fig. (1).** (**A**) Color change of the plant extract during gAgNPs synthesis, which revealed the formation of AgNPs during 24 h. (**B**) UV-vis spectroscopy showed a broad peak between 400-450 nm by UV-vis spectrum, confirming gAgNPs formation. (*A higher resolution/colour version of this figure is available in the electronic copy of the article*).

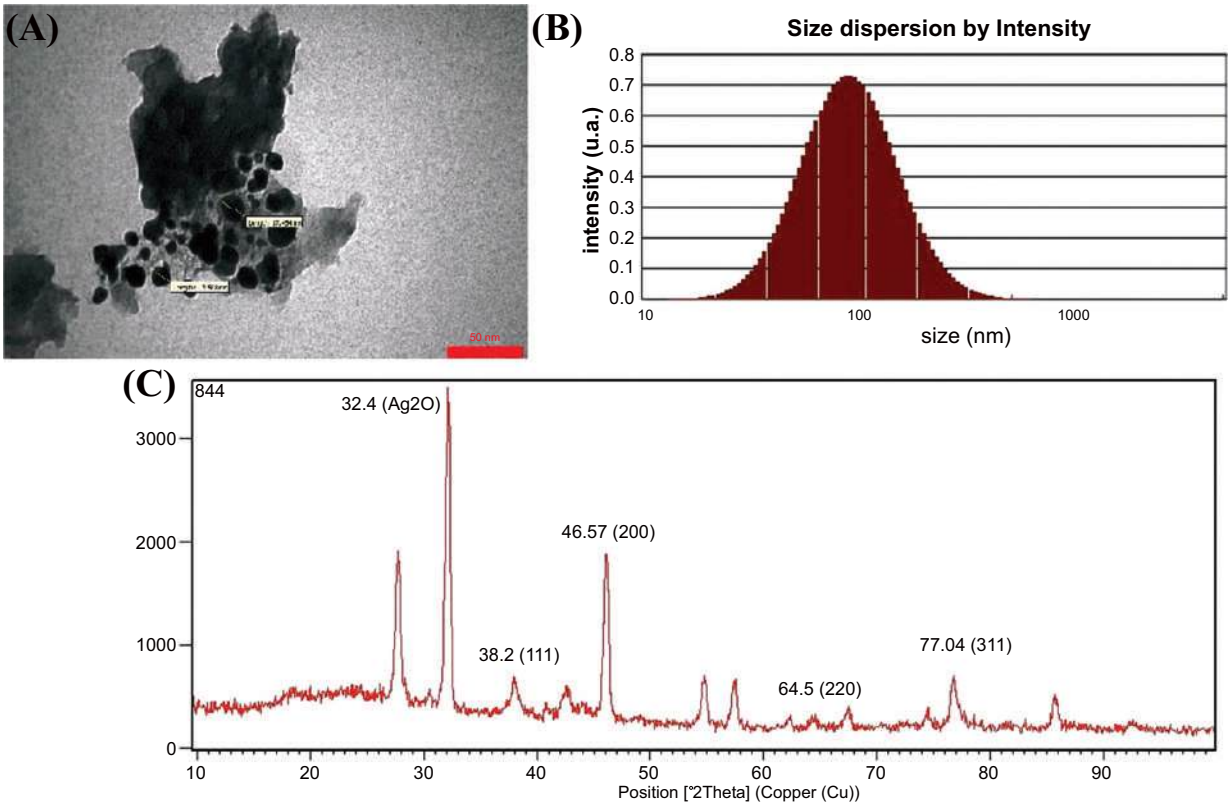


**Fig. (2).** TEM images (**A**), Size distribution (**B**), and XRD spectra (**C**). These physicochemical characterizations confirm nanosized, spherical shape, uniform dispersity, and formation of the face-centered cubic structure of AgNPs. (*A higher resolution/colour version of this figure is available in the electronic copy of the article*).

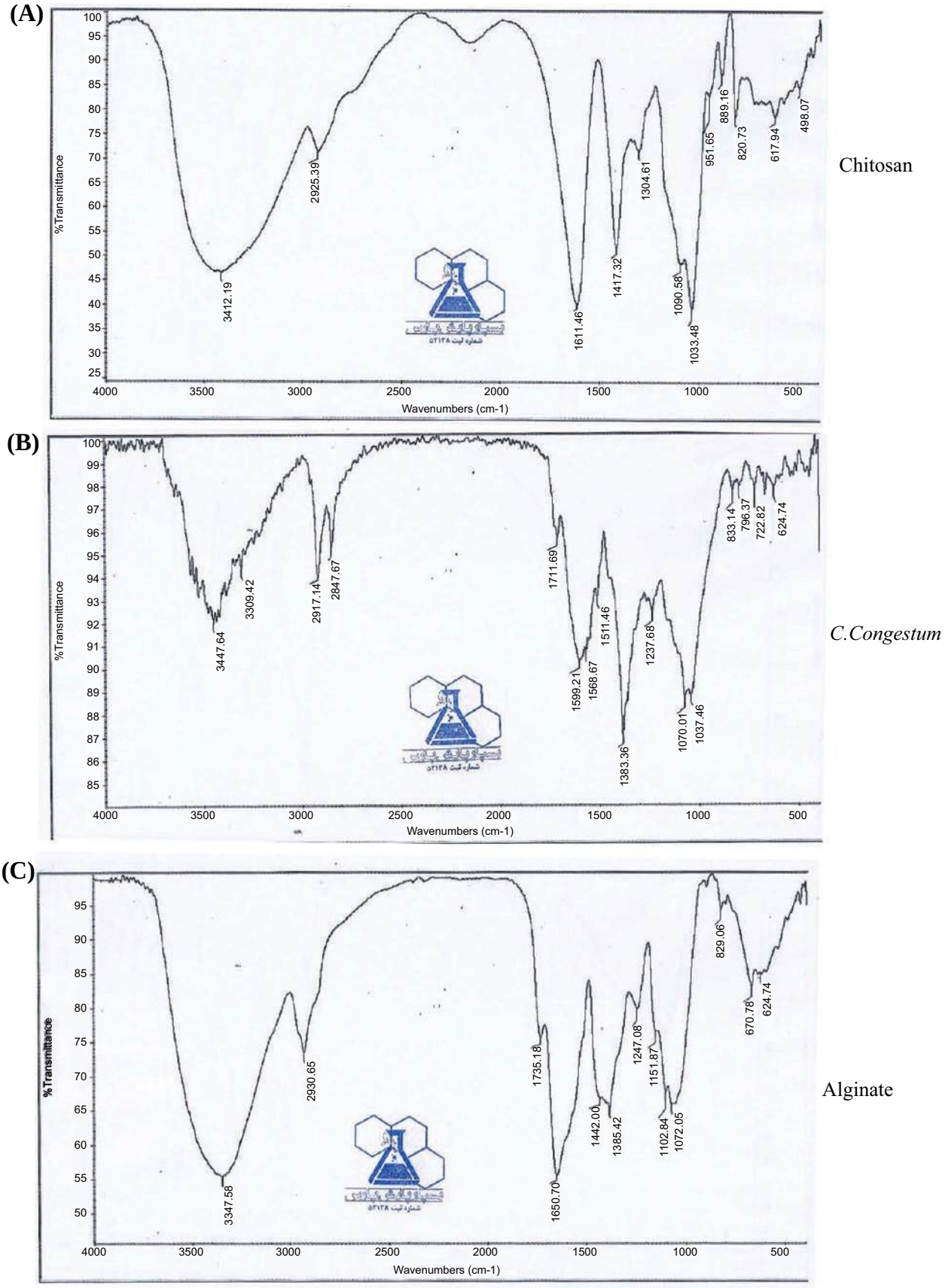
(A)
%Transmittance
Wavenumbers (cm-1)
3412.19
2925.39
1611.46
1417.32
1304.61
1090.58
1033.48
951.65
889.16
820.73
617.94
498.07
Chitosan
(B)
%Transmittance
Wavenumbers (cm-1)
3447.64
3309.42
2917.14
2847.67
1711.69
1599.21
1568.67
1511.46
1383.36
1237.68
1070.01
1037.46
833.14
796.37
722.82
624.74
C.Congestum
(C)
%Transmittance
Wavenumbers (cm-1)
3347.58
2930.65
1735.18
1650.70
1442.00
1385.42
1247.08
1151.87
1102.84
1072.05
829.06
670.78
624.74
Alginate

**(Fig. 3) Contd….**

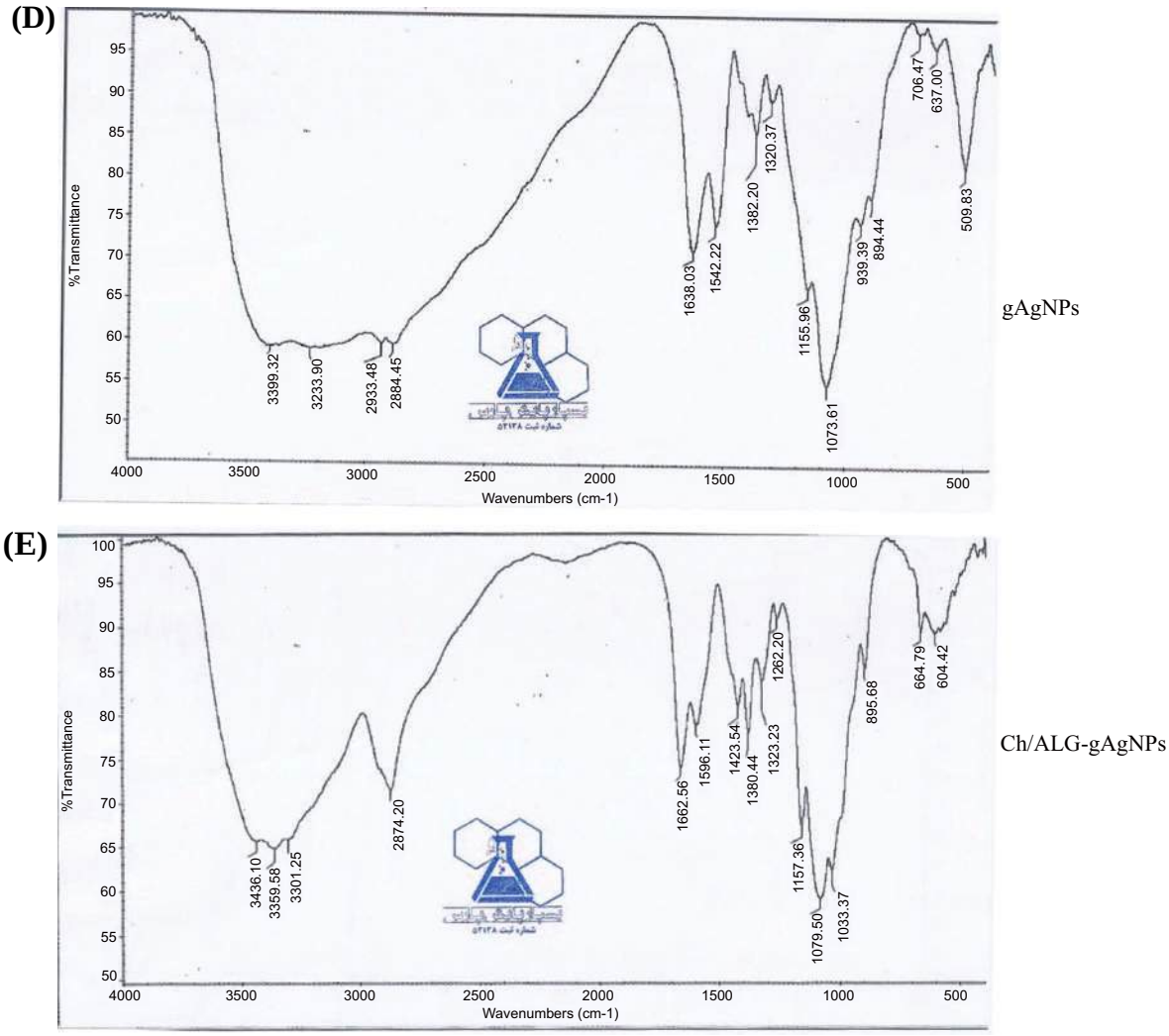


**Fig. (3).** FTIR spectra of chitosan (**A**), Sodium alginate (**B**), *C. congestum* extract (**C**), gAgNPs (**D**), and Ch/ALG-gAgNPs (**E**). FTIR results confirmed the involvement of biological substances of C. *congestum* extract and chitosan/alginate in the Ch/ALG-gAgNPs synthesis. (*A higher resolution/colour version of this figure is available in the electronic copy of the article*).

FTIR results confirmed the contribution of *C. congestum* to the nanoparticle synthesis and surface modification of gAgNPs by Ch/ALG (Figs. **3A**-**E**). In the FTIR spectrum of chitosan, alginate, *C. congestum*, gAgNPs, and Ch/ALG-gAgNPs, the broadband peak around 3000-3600 $cm^{-1}$ belonged to -OH and -NH stretching in the chitosan and biological substances of *C. congestum*. Peaks at 2933, 2925, 2917, and 2874 $cm^{-1}$ belonged to the C-H- stretching in all samples. Peaks at 1611, 1638, and 1626 $cm^{-1}$ corresponded to the C=O stretching. Peaks at 1596, 1599, and 1542 $cm^{-1}$ corresponded to N-H vibration. Peaks at 1417, 1452, and 1423 $cm^{-1}$ corresponded to the -CH2 stretching vibration of hydrocarbon chains. Peaks at 1382 and 1380 $cm^{-1}$ were attributed to $NO_{3-}$ vibrations in the spectrum of gAgNPs and Ch/ALG-gAgNPs. The band at 1154 $cm^{-1}$ was assigned to ionic interaction between $NH^{3+}$ groups of CS and $COO^{-}$ of sodium alginate in the spectrum of Ch/ALG-gAgNPs. A sharp peak at 1033 $cm^{-1}$ in the chitosan spectrum significantly decreased in the bounded chitosan in the Ch/ALG-gAgNPs. This peak belonged to the C–OH stretching of secondary alcohols. Peaks at 1070, 1073, 1079, and 1090 belonged to the stretching vibration of C-O-C bounds.

### 3.2. Antibacterial Activity of Ch/ALG-gAgNPs

The antibiotic-resistant strains of *E. coli* and *S. aureus* were tested for the antibacterial properties of the Ch/ALG mixture, cAgNPs, and Ch/ALG-gAgNPs. The antimicrobial efficacy was measured by standard techniques, such as the disc diffusion test, MIC, and MBC approaches. Table **1** displays the findings of the antibacterial properties resulting from the treatments conducted. The zone of inhibition in the presence of various concentrations (0, 50, 100, 200 µg/ml) of treatments is presented in Fig. (**4**). The inhibition zone of 50, 100, and 200 µg/ml of cAgNPs in *S. aureus* was 2, 4, and 7 mm, respectively, and that in *E. coli* was 7, 10, and 15 mm in diameter. Whereas, at these concentrations of Ch/ALG-gAgNPs inhibition, zone diameters were 8, 10, and 17 mm against *S. aureus* and 11, 14, and 20 mm against *E. coli*. No significant antibacterial activity was seen when *S. aureus* and *E. coli* were tested with 50,

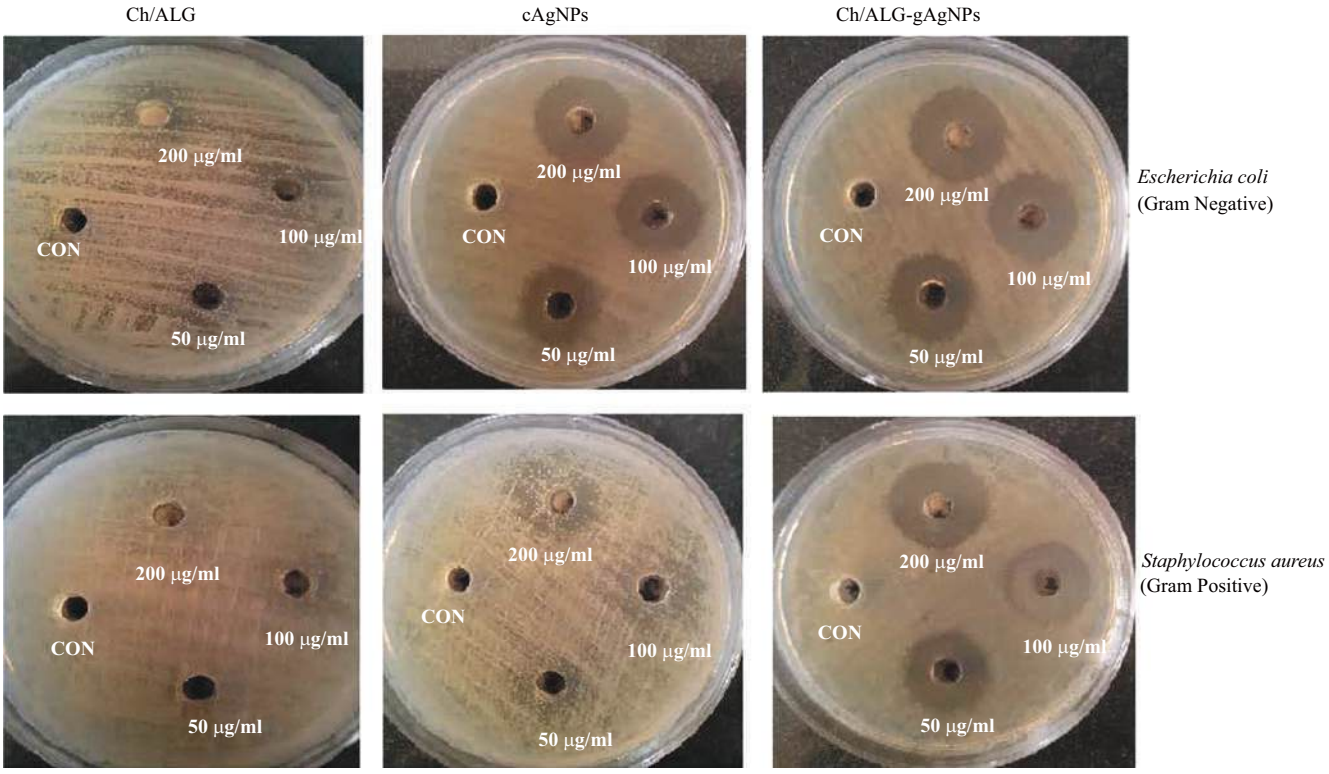


**Fig. (4).** Zone inhibition values (mm) for *E. coli* and *S. aureus* in the presence of different concentrations (50, 100, and 200 µg/mL) of Ch/ALG, cAgNPs, and Ch/ALG-gAgNPs. (*A higher resolution/colour version of this figure is available in the electronic copy of the article*).

**Table 1. Inhibition zone diameter (mm), minimum inhibitory concentration (MIC), and minimum bactericidal concentration (MBC) of Ch-gAgNPs and cAgNPs against resistant strains of *S. aureus* and *E. coli.***

| Treatments | Zone of Inhibition (mm) | | | MIC (µg/ml) | | MBC (µg/ml) | |
|---|---|---|---|---|---|---|---|
| | - | *S. aureus* | *E. coli* | *S. aureus* | *E. coli* | *S. aureus* | *E. coli* |
| Ch/ALG | 0 | - | - | 750 | 500 | 500 | 1000 |
| | 50 µg/ml | 1 | 2 | | | | |
| | 100 µg/ml | 2 | 3 | | | | |
| | 200 µg/ml | 2 | 5 | | | | |
| cAgNPs | 0 | - | - | 125 | 62.5 | 375 | 250 |
| | 50 µg/ml | 2 | 7 | | | | |
| | 100 µg/ml | 4 | 10 | | | | |
| | 200 µg/ml | 7 | 15 | | | | |
| Ch/ALG-gAgNPs | 0 µg/ml | - | - | 62.5 | 15 | 250 | 125 |
| | 50 µg/ml | 8 | 11 | | | | |
| | 100 µg/ml | 10 | 14 | | | | |
| | 200 µg/ml | 17 | 20 | | | | |

100, and 200 µg/ml of Ch/ALG. These zone inhibition findings have been supported by MIC and MBC values. As shown in Table **1**, the MIC value of Ch/ALG, gAgNPs, and Ch/ALG-gAgNPs against resistant *E. coli* was 500, 62.5, and 15 µg/mL, respectively, and against resistant *S. aureus*, it was 750, 125, and 62.5 µg/mL, respectively. As can be seen in Fig. (**5**) and Table **1**, MBC values of Ch/ALG-gAgNPs against *E. coli* (125 µg/mL) and *S. aureus* (250 µg/mL) were less than MBC values of cAgNPs (*E. coli*: 250 µg/mL, *S. aureus*: 375 µg/mL) and Ch/ALG (*E. coli*: 500 µg/mL, *S. aureus*: 1000 µg/mL). These findings indicated that the bactericidal functions of Ch/ALG-gAgNPs for these tested strains were higher than cAgNPs and Ch/ALG solution.

### 3.3. The Effect of Ch/ALG-gAgNPs on Normal Human Cell Viability

MTT tests were used to determine cell viability after 48 hours of incubation with various concentrations (50-200 µg/mL) of cAgNPs or Ch/ALG-gAgNPs. Cell treatment with cAgNPs at concentrations of 12.5 µg/mL (95.8 ± 5.9; relative to non-treated control),

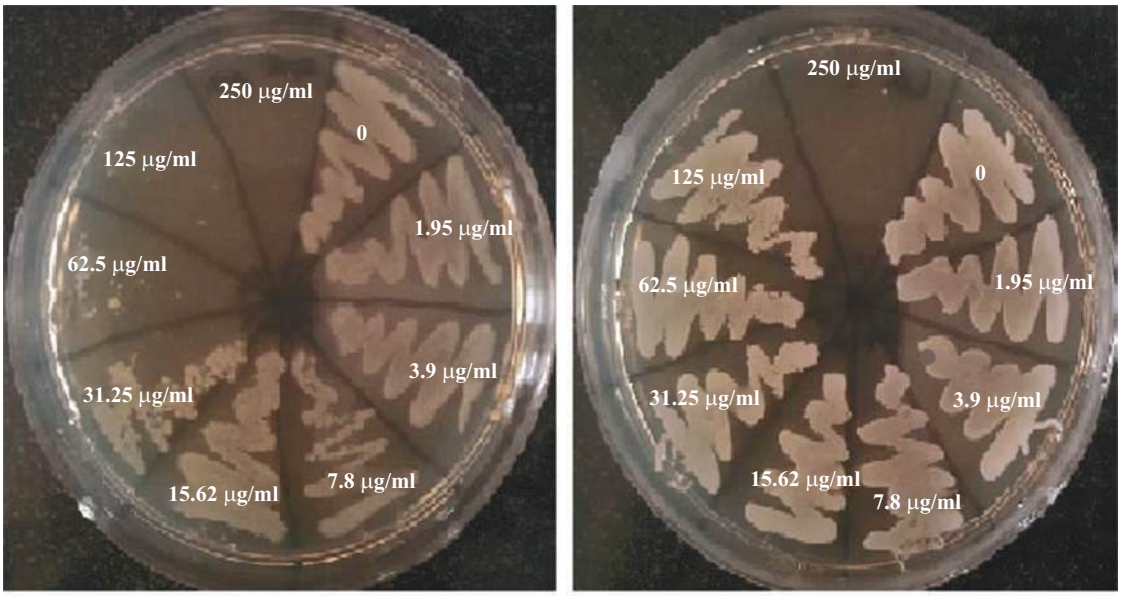


**Fig. (5).** MBC determination of Ch/ALG-gAgNPs *vs*. *E. coli* and *S. aureus.* (*A higher resolution/colour version of this figure is available in the electronic copy of the article*).

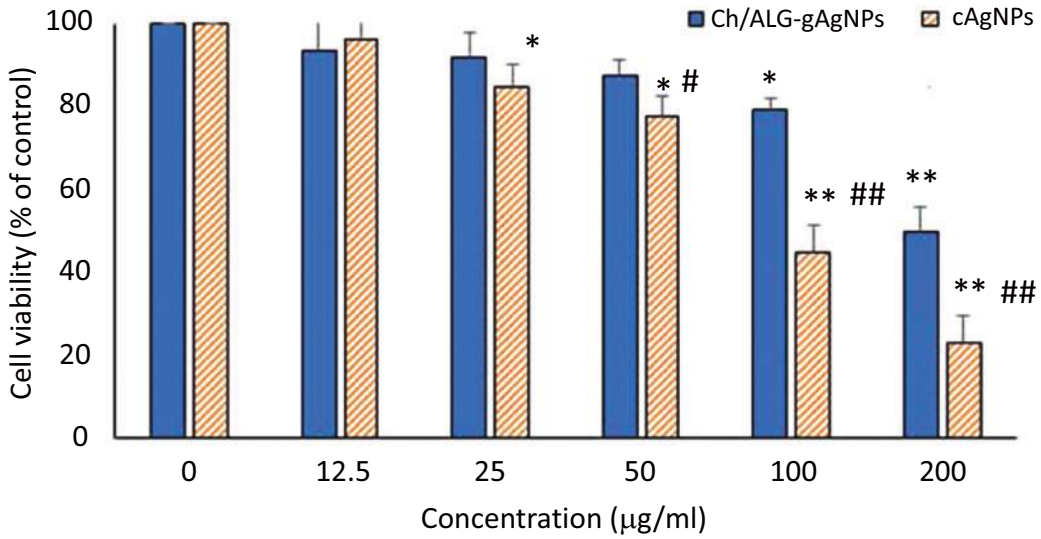


**Fig. (6).** The percentage (%) of cell viability in response to cAgNPs and Ch/ALG-gAgNPs treatment. L929 fibroblast normal cells were incubated with different concentrations (12.5-200 µg/ml) of treatments for 48 h, and cell viability percentage was calculated relative to non-treated control. Experiments were repeated three times and values have been presented as mean ± SD of experiments. In the diagram *($P < 0.01$) and **($P < 0.0001$) represent viability in treated cells *vs*. non-treated cells; #($P < 0.01$) and ## ($P < 0.001$) represent viability of cells in the presence of Ch/ALG-AgNPs *vs*. cAgNPs. (*A higher resolution/colour version of this figure is available in the electronic copy of the article*).

25 µg/mL (84.8 ± 13.07; relative to non-treated control, $P < 0.05$), and 50 µg/mL (77.4 ± 18.8; relative to non-treated control, $P < 0.05$) for 48 hours significantly reduced cell viability of L929 cells. Whereas, treatment with Ch/ALG-gAgNPs at these concentrations (12.5 µg/mL: 93.2 ± 13.2%, 25 µg/mL: 91.73 ± 5.6%, and 50 µg/mL: 87.39 ± 3.7%, relative to non-treated control) showed less cytotoxicity than cAgNPs. MTT findings demonstrated a significant decrease in cell viability of L929 cells after treatment with 100 µg/mL (45.02 ± 6.5 relative to non-treated control (Figs. **6**, **7**); $P < 0.001$) or 200 µg/mL (23.03 ± 6; relative to non-treated control, $P < 0.001$) of cAgNPs. Cell viability percentage at 100 µg/ml (79.13 ± 2.7; relative to non-treated control, $P < 0.05$) and 200 µg/ml (49.73 ± 5.7; relative to non-treated control, $P < 0.001$) of Ch/ALG-gAgNPs was higher than gAgNPs. These findings indicated that Ch/ALG-gAgNPs had low cytotoxic activity at concentrations less than 50 µg/mL and the cytotoxic effect of NPs rose with

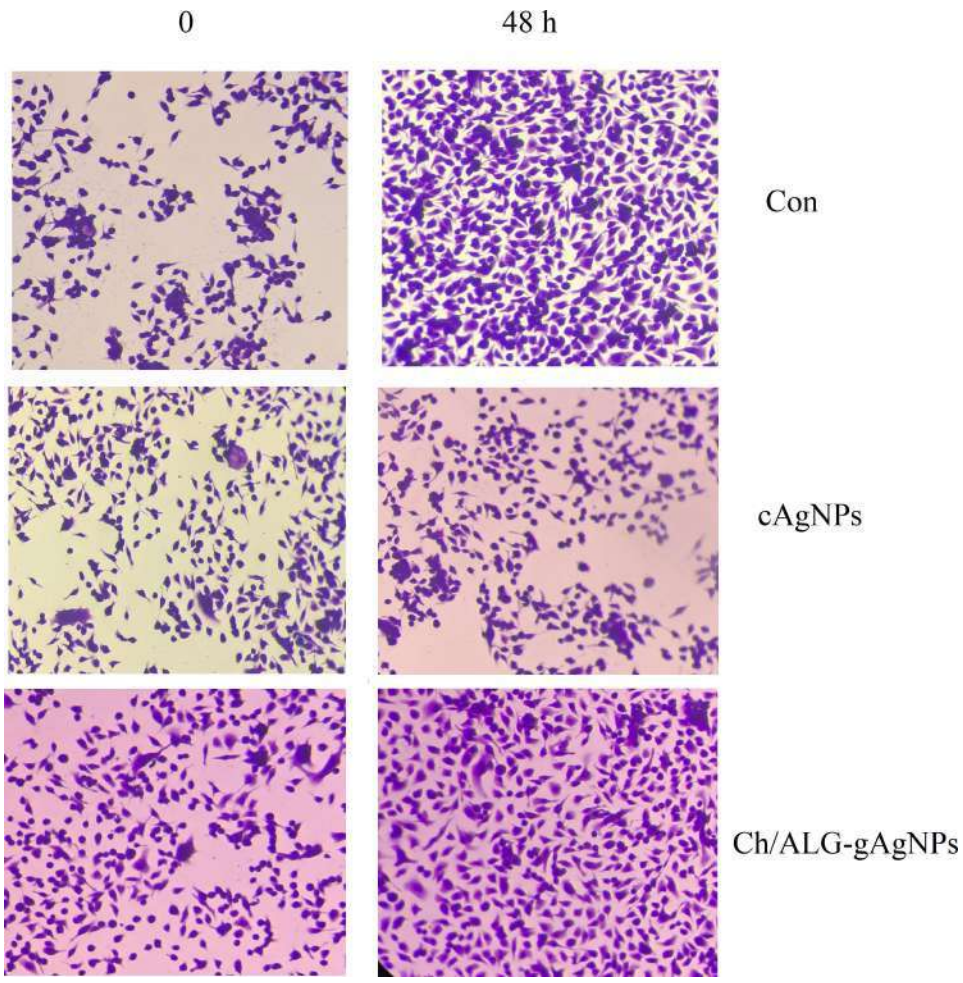


**Fig. (7).** Microscopic images of L929 fibroblast cells treated with 50 µg/mL of cAgNPs and Ch/ALG-gAgNPs after 48 h. (*A higher resolution/colour version of this figure is available in the electronic copy of the article*).

increasing concentration. Therefore, MTT findings showed that green synthesis and surface modification with chitosan decreased the cytotoxic effect of AgNPs on normal human cells. The microscopic images of L929 fibroblast cells after 48 hours of treatment with 50 µg/mL of AgNPs and Ch/ALG-gAgNPs are shown in Fig. (**7**).

### 3.4. Estimation of Cell Apoptosis Markers in the Presence of Ch/ALG-gAgNPs

Flow cytometric analysis confirmed the results of MTT at the concentration of 50 µg/mL. As can be seen in Figs. (**8A-C**), with 50 µg/mL of cAgNPs, the percentage of early apoptosis, late apoptosis, and cell necrosis was 1.2%, 23.6%, and 20.3% respectively. Green synthesis and surface modification changed these values by 0.99%, 14.3%, and 19.2%, respectively. Therefore, the percentage of viable cells in the presence of Ch/ALG-gAgNPs (65.5%) was significantly higher than cAgNPs (54.5%, $P < 0.001$). Fig. (**8**) also shows mRNA expression of pro-apoptotic (BAX) and anti-apoptotic (Bcl-2) markers in the presence of Ch/ALG-gAgNPs and cAgNPs. Cell treatment with 50 µg/mL of cAgNPs markedly suppressed mRNA expression of Bcl-2 and enhanced the expression of BAX relative to the non-treated control. While Ch/ALG-gAgNPs (50 µg/mL) had little effect on mRNA levels of Bcl-2 and BAX markers relative to non-treated control.

## 4. DISCUSSION

AgNPs have shown potential for use in biomedicine as diagnostic or therapeutic agents [7]. However, the cytotoxicity of AgNPs limits the full use of these NPs in biomedicine. The surface chemistry of AgNPs has a significant role in their cytotoxicity on human cells [7, 10, 13, 16]. To overcome this issue, investigators have suggested that surface modification or coating of AgNPs using non-toxic polymers may reduce the cytotoxicity of NPs. Coating of NPs increases their colloidal stability, biocompatibility, and functionalization, and thus improves their safety and efficacy [6, 9, 10, 13, 14]. To benefit from the mentioned consequences, the current study focused on using chitosan and alginate to modify the surface of gAgNPs and their capacity to decrease cytotoxicity in normal cells. The current study has also evaluated the antimicrobial efficacy of Ch/ALG-gAgNPs against pathogenic strains of E. *coli* and *S. aureus*.

In this study, we have synthesized gAgNPs using the green method from *C. congestum* extract, and then the surface of gAgNPs was coated with Chitosan/Alginate polymer (Ch/ALG-gAgNPs). TEM and DLS analysis revealed Ch/ALG-gAgNPs to be near-spherical in shape with a particle size of 50 ± 10 nm. XRD analysis showed a face-centered cubic crystalline structure of Ch/ALG-gAgNPs. FTIR results showed the presence of some

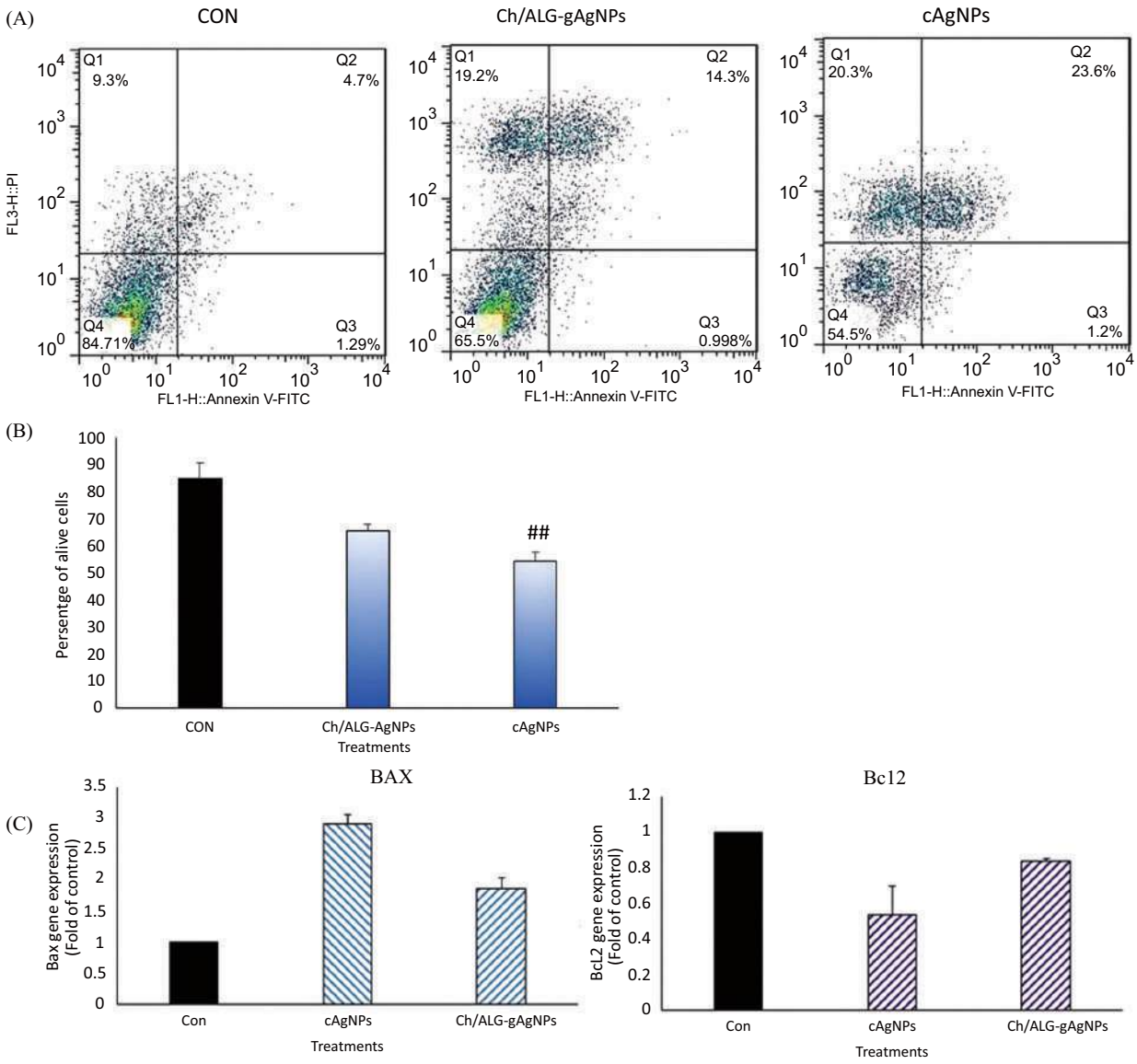


**Fig. (8).** Effect of cAgNPs and Ch/ALG-gAgNPs on L929 cell apoptosis. L929 cells were incubated with 50 µg/mL cAgNPs or CS/ALG-Ag nanocomposite, and were used to determine the alive, apoptotic, and necrotic cell percentages by Annexin V-FITC/ PI staining in conjunction with flow cytometry (**A**). The percentage of alive cells after treatment with cAgNPs and Ch/ALG-gAgNPs. In the diagram, $P < 0.001$ represents the percentage of alive cells in the presence of Ch/ALG-AgNPs *vs*. cAgNPs (**B**). Gene expression analysis of BAX and Bcl2 (**C**). (*A higher resolution/colour version of this figure is available in the electronic copy of the article*).

bioactive compounds of *C. congestum* on the surface of gAgNPs and also confirmed that gAgNPs were successfully conjugated with chitosan/alginate.

The widespread use of silver NPs has raised safety concerns [8]. Metal-based NPs, such as AgNPs, can adversely affect biomolecules in normal mammalian cells [44]. These particles induce cellular apoptosis and necrosis by interacting with vital molecules, such as protein, DNA, and enzyme, generating Reactive Oxygen Species (ROS) and destructing mitochondria [7, 8, 45-47]. The toxic effects of NPs are mainly attributed to their surface physical-chemistry characteristics, such as chemical composition, and electronic and aggregative properties [8, 48]. Green synthesis of AgNPs by crude extracts of microorganisms and plants significantly reduced the cytotoxicity of NPs [47, 48]. In the green or biosynthesis approaches, various biologic substances present in the extracts, such as amino acids, enzymes, alkaloids, tannins, phenolics, proteins, vitamins, and polysaccharides, are responsible for the reduction of $Ag^{+}$ into AgNPs [49, 50].

In the green synthesis of AgNPs, biologic compounds act as capping mediators, form a safe layer of substances on nanoparticle surfaces, and prevent nanoparticle aggregation in biological media [43, 51, 52]. In numerous studies, an increase in safety has been reported through green synthesis of AgNPs using other plant extracts [53-56]. To our knowledge, there has been no study on the cytotoxicity of green synthesized AgNPs (gAgNPs) using *C. congestum* extract. In the current study, the biosynthesis of AgNPs using

*C. congestum* extract significantly increased the safety of NPs. A recent study by Karimian *et al.* demonstrated the biosynthesis of stable and uniform AgNPs using leaf extract of *C. congestum* as a reducing agent. However, no findings regarding cell cytotoxicity have been reported [57].

Surface charge and a release of silver ions are crucial mechanisms for the cytotoxicity of AgNPs [58, 59]. Surface coating can alter the surface chemistry of nanoparticles, stabilize AgNPs by charge repulsion, and inhibit particle aggregation [6, 9, 13, 58]. It can also prevent the release of silver ions from AgNPs [14, 58]. Therefore, it can be proposed that inhibiting particle aggregation and releasing silver from surface modified-AgNPs can significantly decrease their cytotoxicity. Several studies have been conducted by researchers worldwide to reduce AgNPs cytotoxicity after their surface coating with distinctive substances [9, 14, 16]. Our findings have shown coating of gAgNPs with chitosan/alginate to significantly decrease their toxic effects on normal cells compared to cAgNPs. Previously, we have also revealed the surface coating of gAgNPs synthesized using *Spirulina* extracts by chitosan polymer to increase their safety in normal cells [42]. Researchers have supposed that AgNPs drive their cell toxicity by inducing cell apoptosis and necrosis [60, 61]. They believed that AgNPs accumulation and oxidation of $Ag^{+}$ in living cells increase Reactive Oxygen Species (ROS) production, induce oxidative stress, and finally lead to apoptosis-mediated cell death [8, 25, 46, 60]. Our results have also demonstrated that surface modification of gAgNPs by chitosan/alginate markedly decreased cell apoptosis percentage and increased mRNA expression of the anti-apoptotic protein (Bcl2) and attenuated gene expression of the pro-apoptotic protein (Bax2) compared to uncoated particles. Notably, the cell apoptosis reduction in response to the coating of NPs has been reported previously in ours and other studies [25, 43, 62-66].

As seen in our results, Ch/ALG alone exhibited a diminished antibacterial effect, whereas under modified conditions (Ch/ALG-gAgNPs), it enhanced the efficacy of cAgNPs. Research has revealed that polymers usually do not have intrinsic bactericidal activity, except chitosan, which has been introduced as an antimicrobial agent [67]. Under modified conditions, Ch/ALG improved the binding of nanoparticles to bacterial cells, stabilized silver dispersions, and increased their ability to enter and accumulate into cells by interaction with biomolecules on the cell surface [6, 13, 43]. All this has caused the antibacterial ability of modified nanoparticles to be higher than the unmodified ones. In addition, studying the molecular interactions between nanoparticles and bacterial or mammalian cells could enhance our understanding of Ch/ALG-gAgNPs' antibacterial activity and reduced cytotoxicity. Consistent with our findings, Jiang *et al*. [68] reported that coating the nanostructure with hydrophilic polymers did not change their affinity to mammalian cells, but it promoted their bactericidal potential. These findings were attributed to different lipid compositions in bacterial and mammalian cells. The multivalent interactions of amphiphilic nanoparticles and intrinsic curvatures of the membrane lipids provide the required structural rigidity to bend the membrane and reduce pore formation. Due to different lipid and peptide compositions in bacterial and mammalian membrane cells, intrinsic curvatures of the membrane lipids are different. So, mammalian membranes are laden with zero-intrinsic curvature lipids, while microbial membranes are rich in negative intrinsic curvature lipids. The negative intrinsic curvature lipids reduce the energy cost to induce pore formation in the bacterial cells, whereas the energetic barrier is critically high for mammalian membranes laden with zero intrinsic curvature lipids. Therefore, hydrophilic nanoparticles, such as Ch/ALG-gAgNPs, selectively disrupt bacterial membranes, while sparing mammalian cells [68].

The limited access to normal human cells and bacterial strains is the most important limitation of the current study, which can be considered in future studies. In addition, future research can also focus on investigating the long-term cytotoxic effects on humans, scalability, stability, and regulatory aspects that are important for using Ch/ALG-gAgNPs in clinical applications.

## CONCLUSION

The current investigation has demonstrated a simple, low-cost, and eco-friendly approach for green synthesis of gAgNPs using extracts of *C. congestum* modified by chitosan to synthesize CS/ALG-gAg nanocomposites. Ch/ALG-gAgNPs showed a good bactericidal effect against antibiotic-resistant/sensitive strains of *E. coli* and *S. aureus*. Ch/ALG-gAgNPs showed no significant toxic effect against normal cells. The good antibacterial activity with lower toxicity against normal cells makes Ch/ALG-gAgNPs a suitable candidate for use in medical fields.

## LIST OF ABBREVIATIONS

| | | |
|---|---|---|
| AgNPs | = | Ag Nanoparticles |
| TPP | = | Tripolyphosphate |
| Ch/ALG | = | Chitosan/Alginate Mixture |
| UV-Vis | = | Ultraviolet-visible |
| DLS | = | Dynamic Light Scattering |
| MIC | = | Minimum Inhibitory Concentration |
| MBC | = | Minimal Bacterial Concentration |
| OD | = | Optical Density |
| DMEM | = | Dulbecco's Modified Eagle Medium |
| FBS | = | Fetal Bovine Serum |
| ROS | = | Reactive Oxygen Species |

## ETHICS APPROVAL AND CONSENT TO PARTICIPATE

Not applicable.

## HUMAN AND ANIMAL RIGHTS

Not applicable.

## CONSENT FOR PUBLICATION

Not applicable.

## AVAILABILITY OF DATA AND MATERIALS

All data or additional information supporting the results of the current investigation will be available from the corresponding author upon reasonable request.

## FUNDING

Hereby, we extend our gratitude to Neyshabur University of Medical Sciences (project number 140001289, code of ethics IR.NUMS.REC.1401.008).

## CONFLICT OF INTEREST

The authors declare no conflict of interest, financial or otherwise.

## ACKNOWLEDGEMENTS

The authors would like to thank the staff at Islamic Azad University of Neyshabur and Bonab, Neyshabur University of Medical Sciences and Gonabad University of Medical Sciences for their sincere assistance and efforts to make this project happen. This study was supported by funding from grant Dr. Kazemi Ashtiani of the National Elites Foundation.

## REFERENCES

[1] Kadhum WR, Al-Zuhairy SA, Mohamed MB, *et al.* A nanotechnological approach for enhancing the topical drug delivery by newly developed liquid crystal formulations. Int J Drug Deliv Technol 2021; 11: 716-20.

[2] Al-Zuhairy SAS, Kadhum WR, Alhijjaj M, *et al.* Development and evaluation of biocompatible topical petrolatum-liquid crystal formulations with enhanced skin permeation properties. J Oleo Sci 2022; 71(3): 459-68. http://dx.doi.org/10.5650/jos.ess21344 PMID: 35173089

[3] Kadhum WR, See GL, Alhijjaj M, *et al.* Evaluation of the skin permeation-enhancing abilities of newly developed water-soluble self-assembled liquid crystal formulations based on hexosomes. Crystals 2022; 12(9): 1238-45. http://dx.doi.org/10.3390/cryst12091238

[4] Budi HS, Jameel Al-azzawi MF, Al-Dolaimy F, *et al.* Injectable and 3D-printed hydrogels: State-of-the-art platform for bone regeneration in dentistry. Inorg Chem Commun 2024; 161(3): 112026. http://dx.doi.org/10.1016/j.inoche.2024.112026

[5] Soteyome T, Thedkwanchai S. Encapsulation of aromatic coconut water with sodium alginate and calcium chloride. Caspian J Environ Sci 2024; 22: 221-38.

[6] Mulenos MR, Lujan H, Pitts LR, Sayes CM. Silver nanoparticles agglomerate intracellularly depending on the stabilizing agent: implications for nanomedicine efficacy. Nanomaterials 2020; 10(10): 1953. http://dx.doi.org/10.3390/nano10101953 PMID: 33007984

[7] Xu L, Wang YY, Huang J, Chen CY, Wang ZX, Xie H. Silver nanoparticles: Synthesis, medical applications and biosafety. Theranostics 2020; 10(20): 8996-9031. http://dx.doi.org/10.7150/thno.45413 PMID: 32802176

[8] Mao BH, Tsai JC, Chen CW, Yan SJ, Wang YJ. Mechanisms of silver nanoparticle-induced toxicity and important role of autophagy. Nanotoxicology 2016; 10(8): 1021-40. http://dx.doi.org/10.1080/17435390.2016.1189614 PMID: 27240148

[9] Abramenko N, Semenova M, Khina A, *et al.* The toxicity of coated silver nanoparticles and their stabilizers towards *Paracentrotus lividus* sea urchin embryos. Nanomaterials 2022; 12(22): 4003. http://dx.doi.org/10.3390/nano12224003 PMID: 36432289

[10] Das B, Tripathy S, Adhikary J, *et al.* Surface modification minimizes the toxicity of silver nanoparticles: An *in vitro* and *in vivo* study. J Biol Inorg Chem 2017; 22(6): 893-918. http://dx.doi.org/10.1007/s00775-017-1468-x PMID: 28643149

[11] Al-Shik LA, Alshirifi AN, Alkaim AF. Preparation of highly efficient new poly sodium alginate (acrylic acid-co-acrylamide) grafted ZnO/CNT hydrogel nanocomposite: Application adsorption of drug, isotherm and thermodynamics. Caspian J Environ Sci 2023; 21: 865-74.

[12] Alhattab ZD, Aljeboree AM, Jawad MA, Sheri FS, Obaid Aldulaim AK, Alkaim AF. Highly adsorption of alginate/bentonite impregnated TiO2 beads for wastewater treatment: Optimization, kinetics, and regeneration studies. Caspian J Environ Sci 2023; 21: 657-64.

[13] Hirn S, Semmler-Behnke M, Schleh C, *et al.* Particle size-dependent and surface charge-dependent biodistribution of gold nanoparticles after intravenous administration. Eur J Pharm Biopharm 2011; 77(3): 407-16. http://dx.doi.org/10.1016/j.ejpb.2010.12.029 PMID: 21195759

[14] Umut EJ. Surface modification of nanoparticles used in biomedical applications. Mater Sci 2013; 20: 185-208.

[15] Travan A, Pelillo C, Donati I, *et al.* Non-cytotoxic silver nanoparticle-polysaccharide nanocomposites with antimicrobial activity. Biomacromolecules 2009; 10(6): 1429-35. http://dx.doi.org/10.1021/bm900039x PMID: 19405545

[16] Fahmy HM, Mosleh AM, Elghany AA, *et al.* Coated silver nanoparticles: Synthesis, cytotoxicity, and optical properties. RSC Advances 2019; 9(35): 20118-36. http://dx.doi.org/10.1039/C9RA02907A PMID: 35514687

[17] Bilal M, Rasheed T, Iqbal HMN, Li C, Hu H, Zhang X. Development of silver nanoparticles loaded chitosan-alginate constructs with biomedical potentialities. Int J Biol Macromol 2017; 105(Pt 1): 393-400. http://dx.doi.org/10.1016/j.ijbiomac.2017.07.047 PMID: 28705499

[18] Kean T, Thanou M. Biodegradation, biodistribution and toxicity of chitosan. Adv Drug Deliv Rev 2010; 62(1): 3-11. http://dx.doi.org/10.1016/j.addr.2009.09.004 PMID: 19800377

[19] Abd El-Hack ME, El-Saadony MT, Shafi ME, *et al.* Antimicrobial and antioxidant properties of chitosan and its derivatives and their applications: A review. Int J Biol Macromol 2020; 164: 2726-44. http://dx.doi.org/10.1016/j.ijbiomac.2020.08.153 PMID: 32841671

[20] Confederat LG, Tuchilus CG, Dragan M, Sha'at M, Dragostin OM. Preparation and antimicrobial activity of chitosan and its derivatives: A concise review. Molecules 2021; 26(12): 3694. http://dx.doi.org/10.3390/molecules26123694 PMID: 34204251

[21] Frank LA, Onzi GR, Morawski AS, *et al.* Chitosan as a coating material for nanoparticles intended for biomedical applications. React Funct Polym 2020; 147: 104459. http://dx.doi.org/10.1016/j.reactfunctpolym.2019.104459

[22] Saravanakumar K, Sathiyaseelan A, Manivasagan P, *et al.* Photothermally responsive chitosan-coated iron oxide nanoparticles for enhanced eradication of bacterial biofilms. Biomater Adv 2022; 141: 213129. http://dx.doi.org/10.1016/j.bioadv.2022.213129 PMID: 36191538

[23] Shahid-ul-Islam , Butola BS, Verma D. Facile synthesis of chitosan-silver nanoparticles onto linen for antibacterial activity and free-radical scavenging textiles. Int J Biol Macromol 2019; 133: 1134-41. http://dx.doi.org/10.1016/j.ijbiomac.2019.04.186 PMID: 31047926

[24] Bharathi D, Ranjithkumar R, Vasantharaj S, Chandarshekar B, Bhuvaneshwari V. Synthesis and characterization of chitosan/iron oxide nanocomposite for biomedical applications. Int J Biol Macromol 2019; 132: 880-7. http://dx.doi.org/10.1016/j.ijbiomac.2019.03.233 PMID: 30940585

[25] Shao C, Yu Z, Luo T, *et al.* Chitosan-coated selenium nanoparticles attenuate PRRSV replication and ROS/JNK-mediated apoptosis *in vitro*. Int J Nanomed 2022; 17: 3043-54. http://dx.doi.org/10.2147/IJN.S370585 PMID: 35832119

[26] Badawy MEI, Lotfy TMR, Shawir SMS. Preparation and antibacterial activity of chitosan-silver nanoparticles for application in preservation of minced meat. Bull Natl Res Cent 2019; 43(1): 83. http://dx.doi.org/10.1186/s42269-019-0124-8

[27] Peng Y, Song C, Yang C, Guo Q, Yao M. Low molecular weight chitosan-coated silver nanoparticles are effective for the treatment of MRSA-infected wounds. Int J Nanomed 2017; 12: 295-304. http://dx.doi.org/10.2147/IJN.S122357 PMID: 28115847

[28] Ghasemi A, Hashemy SI, Azimi-Nezhad M, Dehghani A, Saeidi J, Mohtashami M. The cross-talk between adipokines and miRNAs in health and obesity-mediated diseases. Clin Chim Acta 2019; 499: 41-53. http://dx.doi.org/10.1016/j.cca.2019.08.028 PMID: 31476303

[29] Reddy SG. Alginates a seaweed product: Its properties and applications of alginates. Polymers 2021; 14: 225-40.

[30] Venkatesan J, Lee JY, Kang DS, *et al.* Antimicrobial and anticancer activities of porous chitosan-alginate biosynthesized silver nanoparticles. Int J Biol Macromol 2017; 98: 515-25. http://dx.doi.org/10.1016/j.ijbiomac.2017.01.120 PMID: 28147234

[31] Martins AF, Monteiro JP, Bonafé EG, *et al.* Bactericidal activity of hydrogel beads based on N,N,N-trimethyl chitosan/alginate complexes loaded with silver nanoparticles. Chin Chem Lett 2015; 26(9): 1129-32.

http://dx.doi.org/10.1016/j.cclet.2015.04.032
[32] Mokhena TC, Luyt AS. Electrospun alginate nanofibres impregnated with silver nanoparticles: Preparation, morphology and antibacterial properties. Carbohydr Polym 2017; 165: 304-12. http://dx.doi.org/10.1016/j.carbpol.2017.02.068 PMID: 28363554
[33] Mohammadlou M, Maghsoudi H, Jafarizadeh-Malmiri HJ. A review on green silver nanoparticles based on plants: Synthesis, potential applications and eco-friendly approach. Int Food Res J 2016; 23: 446.
[34] Akhtar MS, Panwar J, Yun YS. Biogenic synthesis of metallic nanoparticles by plant extracts. ACS Sustain Chem Eng 2013; 1(6): 591-602. http://dx.doi.org/10.1021/sc300118u
[35] Hussain I, Singh NB, Singh A, Singh H, Singh SC. Green synthesis of nanoparticles and its potential application. Biotechnol Lett 2016; 38(4): 545-60. http://dx.doi.org/10.1007/s10529-015-2026-7 PMID: 26721237
[36] Iravani S. Green synthesis of metal nanoparticles using plants. Green Chem 2011; 13(10): 2638-50. http://dx.doi.org/10.1039/c1gc15386b
[37] Bao Y, He J, Song K, Guo J, Zhou X. Plant-extract-mediated synthesis of metal nanoparticles. J Chem 2021; 2021: 1-14.
[38] Jalili M, Sharifi AJJ. Chemical composition and antibacterial activities of the essential oil and extract of *Cirsium congestum*. J food sci technol 2023; 13: 53-60.
[39] Khoshhal F, Sharifi A. Investigating iron content, phenolic compounds and antioxidant activity of *Cirsium congestum* extract. Innov Food Sci Emerg Technol 2018; 10: 79-86.
[40] Rezagholizade-Shirvan A, Masrournia M, Najafi FM, Behmadi H. Synthesis and characterization of nanoparticles based on chitosan-biopolymers systems as nanocarrier agents for curcumin: study on pharmaceutical and environmental applications. Polym Bull 2023; 80(2): 1495-517. http://dx.doi.org/10.1007/s00289-022-04095-4
[41] Rezagholizade-Shirvan A, Fathi Najafi M, Behmadi H, Masrournia M. Preparation of nano-composites based on curcumin/chitosan-PVA-alginate to improve stability, antioxidant, antibacterial and anticancer activity of curcumin. Inorg Chem Commun 2022; 145: 110022. http://dx.doi.org/10.1016/j.inoche.2022.110022
[42] Farhadi L, Mohtashami M, Saeidi J, *et al.* Green synthesis of chitosan-coated silver nanoparticle, characterization, antimicrobial activities, and cytotoxicity analysis in cancerous and normal cell lines. J Inorg Organomet Polym Mater 2022; 32(5): 1637-49. http://dx.doi.org/10.1007/s10904-021-02208-6
[43] Ghasemi A, Salari A, Kalantarmahdavi M, Amiryousefi MR. Sodium metabisulfite in dried plum and its cytotoxic effects on K 562 and L 929 normal cell lines. J Food Sci 2022; 87(2): 856-66. http://dx.doi.org/10.1111/1750-3841.16034 PMID: 35067933
[44] Schrand AM, Rahman MF, Hussain SM, Schlager JJ, Smith DA, Syed AF. Metal based nanoparticles and their toxicity assessment. Wiley Interdiscip Rev Nanomed Nanobiotechnol 2010; 2(5): 544-68. http://dx.doi.org/10.1002/wnan.103 PMID: 20681021
[45] Zhang XF, Shen W, Gurunathan S. Silver nanoparticle-mediated cellular responses in various cell lines: an *in vitro* model. Int J Mol Sci 2016; 17(10): 1603. http://dx.doi.org/10.3390/ijms17101603 PMID: 27669221
[46] Zhang J, Wang F, Yalamarty SSK, Filipczak N, Jin Y, Li X. Nano silver-induced toxicity and associated mechanisms. Int J Nanomedicine 2022; 17: 1851-64. http://dx.doi.org/10.2147/IJN.S355131 PMID: 35502235
[47] Zafar S, Zafar A, Jabeen F, Siddiq MA. Biological Synthesis of Silver Nanoparticles and their Biomedical Activity: A Review. Curr Green Chem 2021; 8(3): 222-41. http://dx.doi.org/10.2174/2213346109666211217091042
[48] Adur AJ, Nandini N, Shilpashree Mayachar K, Ramya R, Srinatha N. Bio-synthesis and antimicrobial activity of silver nanoparticles using anaerobically digested parthenium slurry. J Photochem Photobiol B 2018; 183: 30-4. http://dx.doi.org/10.1016/j.jphotobiol.2018.04.020 PMID: 29684718
[49] Ahmed S, Ahmad M, Swami BL, Ikram S. A review on plants extract mediated synthesis of silver nanoparticles for antimicrobial applications: A green expertise. J Adv Res 2016; 7(1): 17-28. http://dx.doi.org/10.1016/j.jare.2015.02.007 PMID: 26843966
[50] Arif R, Uddin R. A review on recent developments in the biosynthesis of silver nanoparticles and its biomedical applications. Med Devices Sens 2021; 4(1): e10158. http://dx.doi.org/10.1002/mds3.10158
[51] Loo YY, Chieng BW, Nishibuchi M, Radu S. Synthesis of silver nanoparticles by using tea leaf extract from *Camellia sinensis*. Int J Nanomedicine 2012; 7: 4263-7. PMID: 22904632
[52] Negi S, Singh V. Algae: A potential source for nanoparticle synthesis. J Appl Nat Sci 2018; 10(4): 1134-40. http://dx.doi.org/10.31018/jans.v10i4.1878
[53] Ovais M, Khalil AT, Raza A, *et al.* Green synthesis of silver nanoparticles *via* plant extracts: Beginning a new era in cancer theranostics. Nanomedicine 2016; 11(23): 3157-77. http://dx.doi.org/10.2217/nnm-2016-0279 PMID: 27809668
[54] Flieger J, Franus W, Panek R, *et al.* Green synthesis of silver nanoparticles using natural extracts with proven antioxidant activity. Molecules 2021; 26(16): 4986. http://dx.doi.org/10.3390/molecules26164986 PMID: 34443574
[55] Shumail H, Khalid S, Ahmad I, Khan H, Amin S, Ullah B. Review on green synthesis of silver nanoparticles through plants. Endocr Metab Immune Disord Drug Targets 2021; 21(6): 994-1007. http://dx.doi.org/10.2174/1871530320666200729153714 PMID: 32727342
[56] Rani N, Singla RK, Redhu R, Narwal S, Sonia , Bhatt A. A review on green synthesis of silver nanoparticles and its role against cancer. Curr Top Med Chem 2022; 22(18): 1460-71. http://dx.doi.org/10.2174/1568026622666220601165005 PMID: 35652404
[57] Karamian R. Green synthesis of silver nanoparticles using *Cuminum cyminum* leaf extract and evaluation of their biological activities. J Nanostruct 2019; 9(1): 74-85.
[58] Anna B, Barbara K, Magdalena O. How the surface properties affect the nanocytotoxicity of silver? Study of the influence of three types of nanosilver on two wheat varieties. Acta Physiol Plant 2018; 40(2): 31. http://dx.doi.org/10.1007/s11738-018-2613-z
[59] Pang C, Zhang P, Mu Y, Ren J, Zhao B. Transformation and cytotoxicity of surface-modified silver nanoparticles undergoing long-term aging. Nanomaterials 2020; 10(11): 2255. http://dx.doi.org/10.3390/nano10112255 PMID: 33203023
[60] Bressan E, Ferroni L, Gardin C, *et al.* Silver nanoparticles and mitochondrial interaction. Int J Dent 2013; 2013: 1-8. http://dx.doi.org/10.1155/2013/312747 PMID: 24101927
[61] Park EJ, Yi J, Kim Y, Choi K, Park K. Silver nanoparticles induce cytotoxicity by a Trojan-horse type mechanism. Toxicol In Vitro 2010; 24(3): 872-8. http://dx.doi.org/10.1016/j.tiv.2009.12.001 PMID: 19969064
[62] Bastos V, Ferreira-de-Oliveira JM, Carrola J, Daniel-da-Silva AL, Duarte IF, Santos C. Coating independent cytotoxicity of citrate-and PEG-coated silver nanoparticles on a human hepatoma cell line. J Environ Sci 2017; 51: 191-201. http://dx.doi.org/10.1016/j.jes.2016.05.028 PMID: 28115130
[63] Wang F, Chen Z, Wang Y, *et al.* Silver nanoparticles induce apoptosis in HepG2 cells through particle-specific effects on mitochondria. Environ Sci Technol 2022; 56(9): 5706-13. http://dx.doi.org/10.1021/acs.est.1c08246 PMID: 35353488
[64] Vuković B, Milić M, Dobrošević B, *et al.* Surface stabilization affects toxicity of silver nanoparticles in human peripheral blood mononuclear cells. Nanomaterials 2020; 10(7): 1390. http://dx.doi.org/10.3390/nano10071390 PMID: 32708883
[65] Khorrami S, Zarrabi A, Khaleghi M, Danaei M, Mozafari MR. Selective cytotoxicity of green synthesized silver nanoparticles against the MCF-7 tumor cell line and their enhanced antioxidant and antimicrobial properties. Int J Nanomedicine 2018; 13: 8013-24. http://dx.doi.org/10.2147/IJN.S189295 PMID: 30568442
[66] Bin-Jumah M, AL-Abdan M, Albasher G, Alarifi S. Effects of green silver nanoparticles on apoptosis and oxidative stress in normal and cancerous human hepatic cells *in vitro*. Int J

Nanomedicine 2020; 15: 1537-48.
http://dx.doi.org/10.2147/IJN.S239861 PMID: 32210550

[67] Olmos D, González-Benito J. Polymeric materials with antibacterial activity: A review. Polymers 2021; 13(4): 613.
http://dx.doi.org/10.3390/polym13040613 PMID: 33670638

[68] Jiang Y, Zheng W, Tran K, *et al.* Hydrophilic nanoparticles that kill bacteria while sparing mammalian cells reveal the antibiotic role of nanostructures. Nat Commun 2022; 13(1): 197.
http://dx.doi.org/10.1038/s41467-021-27193-9 PMID: 35017467